Supersymmetry and a frequentist approach to model analysis

Sam Rogerson
Imperial College London

October 4, 2010

Abstract

With data taking now underway at all the experiments at the Large Hadron Collider, it is important to understand how to interpret the results in the context of searching for New Physics. A frequentist analysis of models of supersymmetry is presented with the initial results from an implementation of minimal supergravity. Consistency is demonstrated with all phenomenological constraints on supersymmetry along with details of future work.

Contents

1 Introduction

With the total integrated luminosity at the LHC increasing, soon one expects to reach the point where the first glimpses of physics beyond the Standard Model become evident. It is important, by this time, to have in place a description of the systems that can model this New Physics and their respective limitations.

Even simple models of New Physics predict only small deviations from Standard Model (SM) processes or signals. To be capable of determining the presence of New Physics one must, therefore, first have a deep understanding of the Standard Model and the backgrounds it predicts to these searches and signals.

A discussion of the motivations for supersymmetric models is presented and basic models are constructed. A brief overview of the generic signals expected for supersymmetry is given.

A frequentist approach to analysing the parameter space of models of New Physics is detailed. Model-specific analysis is discussed along with a sample implemention for the minimal SUper GRAvity (mSUGRA) model of SUperSYmmetry (SUSY). A comparison of the results for this work is given in the context of existing work concerning the Constrained Minimal Supersymmetric Standard Model (CMSSM) as well as standard benchmark points for supersymmetry.

2 The Standard Model

By observing the symmetries that a system conserves one can write down a generalised Lagrangian. Using this method to construct the SM results in a Lagrangian that describes three of the fundamental fields that define the interactions that are observed in nature, namely quantum chromodynamics (QCD, describing the strong force, embedding the symmetry group $SU(3)_{\mathrm{C}}$) and the electroweak sector ($U(1)_{\mathrm{Y}} \times SU(2)_{\mathrm{L}}$). However this Lagrangian does not explain how any particles acquire mass. Because of this it is also required to have a Higgs sector in the Standard Model. This sector is included as a scalar doublet of the $SU(2)_L$ symmetry group and provides the mechanism to explain how the weak gauge bosons acquire mass [1]. Postulating the existence of a Higgs field - with a non-zero vacuum expectation value - ultimately results in spontaneous breaking of the electroweak gauge symmetry introducing mass terms for these bosons in the Lagrangian.

The ability of the SM to predict precise values for electroweak precision observables (EWPOs), such as the W and Z boson masses and cross-sections as well as rare decay processes, provides a starting point in searching for New Physics by analysing the disagreement between predicted and observed values.

2.1 Indicators of New Physics

While the SM has been incredibly successful, there also exist several discrepancies indicating the existence of physics beyond the Standard Model. While some of these are considered "small" corrections to the SM (e.g. the inclusion of massive neutrinos) and one is entirely absent from the theory (i.e. a description of gravity) there are other measurements and inconsistencies that suggest deviations of observables within the scope of the SM, leading to the suggestion of New Physics.

2.1.1 The divergent Higgs mass

While not related to an observable, when calculating the loop corrections to the Higgs mass (see figure 1) a quadratic divergence appears. These loop contributions to the Higgs mass would seem to drive the mass up to the scale at which New Physics becomes apparent,

$$\delta\left(m_H^2\right) \sim \Lambda^2.$$

Where $\delta\left(m_H^2\right)$ is the correction to the Higgs mass and Λ is the energy scale at which New Physics occurs. This introduces what is known as the hierarchy problem: that there is both a high degree of fine tuning

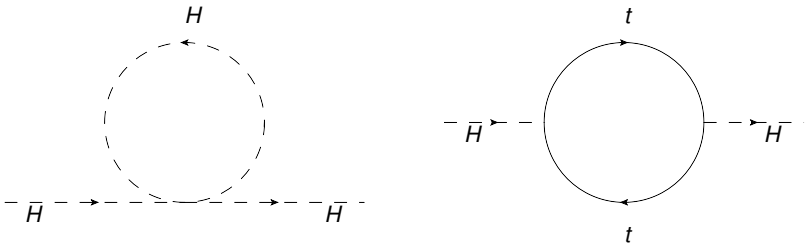

Figure 1: The scalar (left) and fermion (right) single loop corrections to the Higgs mass

required to have reasonable electroweak scale behaviour and that naively this would imply there is no New Physics between the Higgs scale and the unification scale.

2.1.2 Dark matter

Current measurements [2] show a clearly non-zero value for the density of dark matter in the universe (Ω_{CDM}, see table 2). Searches show a value of [3],

$$\Omega_{\mathrm{CDM}}h^2 = 0.1099 \pm 0.0062$$

where Ω_{CDM} is the matter density parameter for cold dark matter (CDM) defined as $\frac{\rho_{\mathrm{CDM}}}{\rho_{\mathrm{crit}}}$ in units h^{-2} where ρ_{crit} is the critical density for the universe, and $h = \frac{H_0}{100km/s/Mpc}$ where H_0 is Hubble's constant. Dark matter is believed to be non-baryonic. As such, any complete theory must provide a candidate particle for dark matter - that is a non-baryonic stable neutral particle. Given that the Standard Model provides no such candidate, and although there is yet to be a direct dark matter detection, this would seem to indicate a level of incompleteness in the Standard Model (if dark matter is successfully directly detected).

A particularly important result of insisting theories provide a candidate dark matter particle is that one expands the scope of measurements which are able to constrain your model. Not only must must the model accurately recreate the standard cosmological measurements (relating to dark matter), but it must also be consistent with the standard cosmology (i.e. not interfering with element abundances [4]).

2.1.3 Anomalous magnetic moments

The anomalous magnetic dipole moment for any particle is calculated from the loop corrections to the magnetic moment of that particle arising from the coupling of it to other particles (as shown in [5]). In the Standard Model the anomalous magnetic moment of a particle is characterised by $g-2$, usually expressed as the parameter a,

$$a = \frac{g-2}{2}$$

with g defined from μ, the magnetic moment,

$$\mu = g\frac{e\hbar}{2m}\frac{S}{\hbar}.$$

where m is the mass of the particle and S is the particle spin.

The anomalous magnetic moment of the electron is one of the most accurately measured (and predicted) observables in particle physics. The degree to which theory and observation agree here [6, 7] is strong evidence for the predictive ability of quantum electrodynamics (QED), and one would expect other measurements from this to be similarly accurate.

Calculating the SM predicted value and measuring a for the muon (a_μ) shows a significant difference [8],

$$a_\mu^{\text{obs}} - a_\mu^{\text{SM}} > 3\sigma.$$

Because these loop corrections arise from any particle with a non-zero coupling to the muon, a_μ is sensitive to contributions from any New Physics particles that fulfil this criterion. This implies, given the huge amount of evidence in support of QED, there exists some beyond-SM particles, which couple to the muon, whose contributions correct this discrepancy.

3 Motivating TeV scale New Physics

While the previous section details why one expects New Physics at *some* point, it is important to understand why one expects to see evidence of New Physics at the TeV scale, which would put it in reach of the LHC.

The strongest indicator of TeV scale new physics comes from the scattering cross-section of the massive vector-bosons. Calculating the perturbative value of $\sigma(WW \to WW)$ shows that the value explodes with increasing energy, violating perturbative unitarity. To stabilise the cross-section and preserve unitarity one needs to include other terms in the calculation to cancel out the divergences; the presence of these terms would need to become apparent at the $\sim$ TeV scale [9]. One method to this end is to include a third propagator to this process (on top of γ and Z^0) in the form of the scalar Higgs boson. In this way the vector-boson scattering cross-section puts limits on both the scale of new physics and the mass of the Higgs.

As described in Section 2.1.1, quadratic loop corrections cause the Higgs mass to diverge without the presence of an exceptional degree of fine tuning at the unified scale (GUT scale). This fine tuning seems unnatural; that is, there seems no motivation for such a degree of fine tuning to exist. To avoid this hierarchy problem the existence of non-Standard Model particles are predicted which cancel out these divergences - implying these are in someway partners to the Standard Model particles (if only through their coupling to the Higgs).

In essence, to solve this discrepancy one must choose some point in the energy scale at which the SM breaks down [10] denoted Q_L. This leaves two possible options,

(i) The SM is the correct description of all physics up to and including the Planck scale[1] implying there should exist some more fundamental theory describing behavior at and above the Planck scale to account for the necessary fine tuning.

(ii) Q_L is chosen to be below the Planck scale, and at Q_L New Physics is introduced that cancels the radiative correction terms.

Since option (i) does little to resolve the other inconsistencies described in Section 2.1 option (ii) would seem more reasonable.

The most significant leading order contributions to the quadratic divergence come from the top quark, due to the top Yukawa coupling (λ_t) being dominant. Given that we expect the new particles to be, in some way, 'partners' to the SM particles (in the most simple case) we would expect them to couple to the Higgs in a similar way. For these partners to have a discernible effect and resolve the divergence problem, New Physics must become apparent at or near the TeV scale or else the corrections would be too heavily suppressed due to the reduced cross-section [10].

This motivates a relatively light top quark , and similarly bottom quark, partner. There were no observations indicating the existence of such particles within the range of either LEP [12] or the TeVatron [13]; this pushes the lower limit on $m_{\tilde{t},\tilde{b}}$ sufficiently high to require a small degree of fine tuning to resolve the divergences, hence creating what is termed the "little hierarchy problem" [14].

[1] if this point, Q_L, is aribitrarily high this results in a non-interacting theory at low energies [11]

4 Models of New Physics

When constructing new models of physics it is important to both recreate current observation and resolve known problems, while minimizing the number of assumptions made.

While many models exist it is prudent to concentrate on those whose assumptions are well motivated and also provide quantatitive signals. Those models that can succesfully resolve several (or all) of the issues presented in Section 2.1 are of particular interest.

As already discussed in Section 3, to resolve the hierarchy problem we need to introduce (at least) a partner to the top quark. There is nothing that indicates the top quark is unique in this regard, and was only used as an example as it gives the most significant contribution, because of this it is not unreasonable to expect New Physics to consist of partners for all of the SM particles. Each SM particle having a partner would suggest the existence of some extra symmetry of the system.

To resolve the dark matter problem (Section 2.1.2) the model must provide a stable neutral non-baryonic particle. Simply introducing a single disconnected candidate particle for CDM is not well motivated and ad hoc. If this is to be resolved through the introduction of partners to the SM particles the lightest of these partners must be stable, implying that decay from the partners to the SM particles is in some way restricted (again motivating the existence of some underlying symmetry in the formation of the model).

Finally, to resolve the discrepancy in the predicted and observed value for the anomalous magnetic moment of the muon (a_μ) one predicts the existence of particles that couple to the muon in such a way that they reduce the value of $a_\mu^{obs} - a_\mu^{theo}$ to statistically acceptable levels. Partners to the SM particles would provide a plausible method for resolving this as it would be expected (even in the simplest case) to have some particles that have a non-zero coupling to the muon.

It would seem that a quite natural solution has arisen that has the possibility of resolving the main inaccuracies of the Standard Model, while a complete model has not been constructed any such model based on these ideas must provide a set of partners to the SM particles with the above properties and most likely incorporate some form of additional symmetry.

It should be noted at this time that there are models that seek to go further than this and resolve not only the above issues but also explicitly attempt the unification of gravity with the other fundamental forces. While the details of these will not be covered here it is relevant to show that even these more complex models provide partners and a similar prescription to that given here.

There are three particularly representative models of the attempts to unify gravity with the other forces: Universal Extra Dimensions (UED), Large Extra Dimension (ADD[2]) and Randall-Sundrum (RS) models. While these all treat gravity in a similar fashion, they have distinctly different approaches to handling of the SM fields. They also share a common ground in having a basis related to Kaluza-Klein theory. Given that all of these models, to some degree, confine the SM fields to some restricted dimension there exists the possibility of standing waves of the SM fields in the dimensions they are confined to, and naively these have the normal mass associated with a wave

$$M = \frac{1}{\lambda_n}\frac{h}{c} = \frac{n}{r}\frac{h}{c},$$

where n is an integer, h is Planck's constant, c is the speed of light, λ_n is a half-integer multiple of the wavelength, and r is the characteristic radius of the dimension to which the field is restricted. Since n is free to vary, this results in what are known as *Kaluza-Klein towers*, that is a periodic sequence of particles with increasing mass. Since these are constructed from standing waves of the SM fields it is apparent subsequent excitations (higher values of n) are partners to the SM particles, and while there is

[2]named for Nima Arkani-Hamed, Savas Dimopoulos, and Gia Dvali [15]

more than one set of partners this is not inconsistent with the arguments presented so far (e.g. resolving divergences).

5 Supersymmetry

Now that the idea of a generation of partners to the SM particles has been motivated, we introduce a specific class of models known as SUperSYmmetry.

In SUSY a symmetry is introduced between bosons and fermions, such that each boson has a fermion partner and vice-versa. This would mean, for example, that the electron has a spin-0 partner named the *selectron*. Other than the spin-$\frac{1}{2}$ difference this particle should have the same mass and quantum numbers as the electron. If this were true, these *s*particles would have been observed in many detectors experiments already. The lack of detection implies that supersymmetry is not an exact symmetry and that at some scale the symmetry breaks down. If the symmetry is strongly broken then this would mean the super-partners (sparticles) can have very high masses and we have to deal with the hierarchy problem again. This leads one to assume that the symmemtry is only weakly broken.

In fact there is already evidence of the degree to which, if it exists, supersymmetry is broken and from this the mass scale at which the sparticles exist. Consider the three coupling constants for each of the forces in the SM, $\alpha_{1,2,3}$. The values of α_i are dependant on the energy scale, μ, and are calculated by solving the *renormalization group equations* (RGEs) which are sensitive to the particles with $M < \mu$ charged with respect to the force. Figures 2(a) and 2(b) show how the α_i scale with μ. The α_i in the supersymmetric theory unify at a scale of $\sim 2 \times 10^{16}$GeV. This unification lends strong evidence toward TeV scale New Physics as in Section 3.

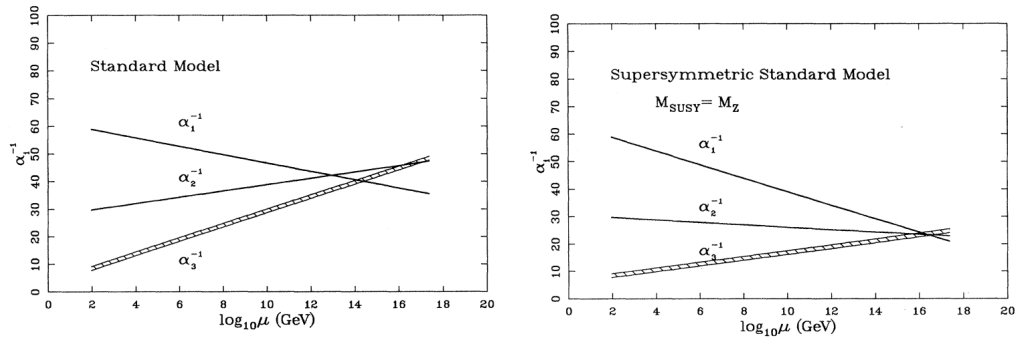

(a) Coupling constants in the SM as a function of energy scale μ

(b) Coupling constants in a weakly broken supersymmetric Standard Model as a function of energy scale μ, with sparticles masses $M \lesssim 1$TeV

Figure 2: From [16].

5.1 The MSSM and CMSSM

The model presented above is termed the Minimal Supersymmetric Standard Model (MSSM). This model also introduces a multiplicatively conserved parity, called R-parity, defined as:

$$R = (-1)^{2j+3B+L}$$

where j is spin, B baryon number and L lepton number. This means that all SM particles have $R = 1$ and all sparticles have $R = -1$, and ensures the lightest supersymmetric partner (LSP) is stable, providing us with the possbility of a reasonable dark matter candidate (see Section 2.1.2). R-parity also enforces reasonable phenomenology at the low energy scale, such as ensuring the stability of the proton.

(s)particles$_{\mathbf{h}}$	spin
$[u,d,c,s,t,b]_{L,R}$ $[e,\mu,\tau]_{L,R}$ $[\nu_{e,\mu,\tau}]_L$	$\frac{1}{2}$
$[\tilde{u},\tilde{d},\tilde{c},\tilde{s},\tilde{t},\tilde{b}]_{L,R}$ $[\tilde{e},\tilde{\mu},\tilde{\tau}]_{L,R}$ $[\tilde{\nu}_{e,\mu,\tau}]_L$	0
g $(W^{\pm},H^{\pm})$ (γ,H_1^0,H_2^0)	1 / 0
$\tilde{g}$ $\tilde{\chi}_{1,2}^{\pm}$ $\tilde{\chi}_{1,2,3,4}^0$	$\frac{1}{2}$

Table 1: The minimal supersymmetric Standard Model (s)particles, h signifying handedness, $H_{1,2}^0$ are the Higgs doublets.

On top of partners to the SM particles supersymmetry also predicts an enlarged Higgs sector, consisting of two Higgs doublets, resulting in five physical Higgs particles - h^0,H^0,A^0,$H^{\pm}$ (see table 1 for the full list of particles).

With the introduction of sparticles, our theory is now characterised by many more parameters than it was before. The SM could be uniquely defined by 19 parameters, whereas for the MSSM we require *at least* 105. This would seem to suggest that there is a degree of "unnaturalness" to the theory and that the true underlying theory has not yet been realised. A second, more practical problem, is that with 105 free parameters any sort of investigation of the parameter space with reasonable coverage is computationally expensive. One can, however, impose reasonable conditions on the MSSM to reduce this parameter space.

The Constrained Minimal Supersymmetric Model (CMSSM) reduces the number of parameters by enforcing universality at a scale *above* the renormalisation scale, in turn reducing the free parameters to the scalar mass m_0, the gaugino mass $m_{\frac{1}{2}}$, the trilinear coupling A_0, $\tan\beta$ (where $\tan\beta$ is the ratio of the two neutral Higgs field vacuum expectation values) and finally the sign of μ, the Higgs mixing parameter [17]. The universality condition states that, at the high scale, all of the scalar masses of squarks, sleptons and the Higgs fields ($m_{h_{1,2}}$) are equal to m_0, the gaugino masses are equal to $m_{\frac{1}{2}}$, and the trilinear couplings are related by A_0 to the Yukawa couplings λ_f [18].

5.2 mSUGRA

Minimal SUper GRAvity (mSUGRA) is more tightly constrained than the CMSSM. At the unification (GUT) scale it imposes a relationship between B_0 (the bilinear Higgs coupling), A_0 (the trilinear coupling) and $m_{3/2}$ (the mass of the gravitino, super partner of the graviton),

$$B_0 = A_0 + m_{3/2}$$

with the aim being to remove the "by hand" unification of the CMSSM. In supergravity models the scalar masses are automatically universal [19]. At the GUT scale,

$$m_0^2 = m_{3/2}^2 + \Lambda$$

where Λ is the cosmological constant. If we assume $\Lambda = 0$ then $m_{3/2} = m_0$ and our boundary condition becomes

$$B_0 = A_0 + m_0$$

Unlike the CMSSM, mSUGRA imposes a specific GUT scale boundary condition. While, as noted, this results in unversality, one loses the ability to vary some of the weak scale parameters [20] and the model is now entirely constrained by m_0, $m_{\frac{1}{2}}$, A_0 and the sign of (μ).

6 A brief introduction to searches for supersymmetry

Now that SUSY models which have reasonable numbers of parameters have been constructed, and still embed the overall behaviour of SUSY models, it is important that direct and indirect observable effects of these models are defined. These observables, as expected, cover a broad range of physics (cosmological values, b-physics, electroweak precision measurements, etc.) and in some cases are exceptionally sensitive to New Physics. A large sample of the more commonly considered observables can be found in table 2.

Any constraint that one implements is model specific, and in some cases some models cannot be easily distinguished (for example technicolor and extradimensional theories are indistinguishable in some regions of their parameter spaces [21]). It is important then not to become too model focused and look at the general signals of SUSY. There are some direct observations that arise out of SUSY phenomenology; namely missing transverse energy in an event (missing E_T, see Section 6.1) and same sign dileption events (see Section 6.3).

6.1 Missing transverse energy

This is a particularly promising channel to search for signals of SUSY models (that is pp $\rightarrow$ jets $+ ME_T$ where E_T is the transverse energy), but *only* those derived from the MSSM or others that enforce R-parity conservation. Because of multiplicative R-parity conservation sparticles in the MSSM can only be pair-produced from SM particles, and decay until the LSP is reached, which is usually considered to be a neutralino, $\tilde{\chi}_1^0$. These particles escape the detector, so would manifest themselves as missing transverse energy. This is an attractive feature of these models as this must occur for *all* R-parity conserving models (and models with similar conservation laws); this allows any other analysis to be combined with missing E_T. The missing energy should correspond to a particular range of possible masses for the sparticles escaping the detector and therefore can be related to the indirect constraints on the sparticle masses from other experiments and observations.

Figure 3 clearly shows that as the event's missing E_T increases the SM background processes fall off, leaving a comparatively clear signal.

6.2 Opposite sign dilepton events

A particularly well studied possible neutralino decay to leptons and the LSP is $\tilde{\chi}_2^0 \rightarrow \ell^{\pm}\ell^{\mp}\tilde{\chi}_1^0$. Combining this signal with a study of missing E_T theory predicts a linear rise, with energy, of the invariant mass spectrum of the leptons that abruptly cuts off at the kinematic limit characterised by the mass difference between the two neutralinos. This edge gives a distinct direct observable to SUSY, and while in current experiment this would not be used as a measurement of the mass-splitting, it does act as a possible "discovery-signal". The position of this edge can be theoretically calculated with relatively high precision [22].

6.3 Same sign dilepton events

While in the SM a large number of events are only allowed with leptons being produced in $\ell^{\pm}\ell^{\mp}$ pairs (e.g. $Zbb \rightarrow llbb$, $t\bar{t}$ events, $WW +$ jets, etc. [23]) there is a much greater cross-section for processes resulting in same sign ($\ell^{\pm}\ell^{\pm}$) lepton production in SUSY. This attribute makes the same sign dilepon signal a comparatively low-background channel (with the main background arising from QCD dijet production, top quark production, and electroweak boson production [24]).

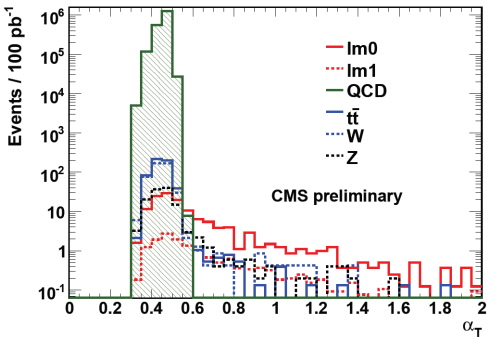

Figure 3: Standard model backgrounds shown against the supersymmetry signal (at the standard survey points in parameter space named $lm0$ and $lm1$, see Section 7.1.3 for details) in an n-jet event for varying α_t [25], which embeds the *balance* of the jets in the event, i.e. for a completely balanced event $\alpha_t = 0.5$ and one would expect either no missing energy or (for a dijet event) equal loss. Cutting on $\alpha_t > 0.6$ in this situation would elimate the majority of the background (QCD).

7 Model Fitting and `MasterCode`

Irrelevant of the choice of model it is necessary to understand how consistently that model recreates known phenomology at the weak scale. This requires a statistical measure of consistency.

There are two fundamentally different approaches; Bayesian and frequentist interpretation of probability. The Bayesian view is the probability of a hypothesis H, given some data D, can be estimated even given incomplete knowledge of the population and system, i.e. $P(H|D) = \frac{P(D|H)P(H)}{P(D)}$, where $P(H)$ is the probability of the hypothesis prior to the data, $P(D)$ is the probability of the data, $P(D|H)$ is the probability of the data D given the hypothesis H is true and $P(H|D)$ is the probability of the hypothesis being true once the data D has been seen. The frequentist approach is to interpret probability as the expected "frequency of occurence" of an event defined by the hypothesis, that is

$$P(A) = \lim_{n_t \to \infty} \frac{n_A}{n_t}, \tag{1}$$

where n_A is the number of events defined by A and n_t is the total number of events.

The Bayesian approach has the advantage that once calculated one can make statements such as "there is a 95% probability that this region contains the *mean* of the distribution", however this is always controlled by the specification of the priors (i.e. $P(H)$). The advantage of the frequentist interpretation is that one is only concerned with the *sample* mean and is unconcerned with priors. The frequentist approach is limited to making statements such as "95% of similar intervals would contain the *true* mean".

To decide between a Bayesian and frequentist approach to model analysis, one must be pragmatic. The main critcism of the frequentist interpretation comes from the defintion of probability (see (1)) relying on the limit $n_t \to \infty$ where in reality one can only have a finite sequence of events. For a Bayesian approach to be successful the resulting confidence level calculation cannot be dependant on the specification of the prior. Since there is no obvious way of confidently understanding the priors for all supersymmetric models (i.e. specifying a probability of the hypothesis itself being true), and there is evidence that the calculations are sensitive to the choice of priors for at least some models [26], it would seem to be more consistent to use a frequentist approach. Also, when presented with a well sampled parameter space whose dependant variables are smoothly varying and define the likelihood at a given point, it becomes reasonable to assume the sample mean is in fact the true mean.

There are of course problems with implementing a frequentist approach. The frequentist calculation of a confidence level only takes into account the *precise* model that you are analysing and leaves no room for small additions or changes that may not affect the underlying model but do make it more consistent with the statistical constraints. This means that each model and variation of model must be individually visited and analysed. Particularly when dealing with large parameter spaces this can be computationally intensive task to ensure full coverage and therefore justify the frequentist intepretation.

The aim of the approach presented is to cover the entire GUT scale parameter space of a given model and calculate the values of various low energy parameters that it predicts at each point. These can then act as a constraint for the model against the current best values from experiment.

These ideas are what motivated the development of `MasterCode` [17]. This is developed by a collaboration involving both experimentalists and theorists in an attempt to ensure consistent and accurate interpretation and implementation of the constraints and their errors. One defines a global χ^2 likelihood

Observable	Th. source	Ex. Source	Constraint	Add. Th. Unc.
m_t[GeV]	[27, 28]	[29]	173.1 ± 1.3	-
$\Delta\alpha^{(5)}_{\rm had}(m_z)$	[27, 28]	[30]	0.02758 ± 0.00035	-
M_Z[GeV]	[27, 28]	[30]	91.1875 ± 0.0021	-
Γ_Z[GeV]	[27, 28]	[30]	2.4952 ± 0.0023	0.001
$\sigma^0_{\rm had}$[nb]	[27, 28]	[30]	41.540 ± 0.037	-
R_l	[27, 28]	[30]	20.767 ± 0.025	-
$A_{\rm fb}(\ell)$	[27, 28]	[30]	0.01714 ± 0.00095	-
$A_\ell(P_\tau)$	[27, 28]	[30]	0.0465 ± 0.0032	-
R_b	[27, 28]	[30]	0.21629 ± 0.00066	-
R_c	[27, 28]	[30]	0.1721 ± 0.003	-
$A_{\rm b}(\ell)$	[27, 28]	[30]	0.0992 ± 0.0016	-
$A_{\rm c}(\ell)$	[27, 28]	[30]	0.0707 ± 0.0035	-
A_b	[27, 28]	[30]	0.923 ± 0.020	-
A_c	[27, 28]	[30]	0.670 ± 0.027	-
A_ℓ(SLD)	[27, 28]	[30]	0.1513 ± 0.0021	-
$\sin^2\theta^\ell_W(Q_{\rm fb})$	[27, 28]	[30]	0.2324 ± 0.0012	-
M_W[GeV]	[27, 28]	[31, 32]	80.399 ± 0.025	0.010
$\mathrm{BR}^{\rm exp}_{b\to s\gamma}/\mathrm{BR}^{\rm SM}_{b\to s\gamma}$	[33, 34, 35, 36, 37]	[38]	$1.117 \pm 0.076_{\rm exp} \pm 0.082_{\rm th(SM)}$	0.050
$\mathrm{BR}(B_s\to\mu^+\mu^-)$	[39, 40, 41, 42]	[38]	$< 4.7 \times 106-8$	0.02×10^{-8}
$\mathrm{BR}^{\rm exp}_{B\to\tau\nu}/\mathrm{BR}^{\rm SM}_{B\to\tau\nu}$	[41, 42, 43]	[44, 45, 46]	$1.25 \pm 0.040_{\rm exp+th}$	-
$\mathrm{BR}(B_d\to\mu^+\mu^-)$	[39, 40, 41, 42]	[38]	$< 2.3 \times 10^{-8}$	0.01×10^{-9}
$\mathrm{BR}^{\rm exp}_{B\to X_s\ell\ell}/\mathrm{BR}^{\rm SM}_{B\to X_s\ell\ell}$	[47]	[38, 47]	0.99 ± 0.32	-
$\mathrm{BR}^{\rm exp}_{K\to\mu\nu}/\mathrm{BR}^{\rm SM}_{K\to\mu\nu}$	[41, 43]	[48]	$1.008 \pm 0.014_{\rm exp+th}$	-
$\mathrm{BR}^{\rm exp}_{K\to\pi\nu\bar\nu}/\mathrm{BR}^{\rm SM}_{K\to\pi\nu\bar\nu}$	[49]	[50]	< 4.5	-
$\Delta M^{\rm exp}_{B_s}/\Delta M^{\rm SM}_{B_s}$	[49]	[42, 51]	$0.97 \pm 0.01_{\rm exp} \pm 0.27_{\rm th(SM)}$	-
$\frac{\Delta M^{\rm exp}_{B_s}/\Delta M^{\rm SM}_{B_s}}{\Delta M^{\rm exp}_{B_d}/\Delta M^{\rm SM}_{B_d}}$	[39, 40, 41, 42]	[38, 52, 51]	$1.00 + 0.01_{\rm exp} \pm 0.13_{\rm th(SM)}$	-
$\Delta\epsilon^{\rm exp}_K/\Delta\epsilon^{\rm SM}_K$	[49]	[52, 51]	$1.08 \pm 0.14_{\rm [exp+th]}$	-
$a^{\rm exp}_\mu - a^{\rm SM}_\mu$	[53, 54, 55, 56]	[57, 58, 59]	$(30.2 \pm 8.8) \times 10^{-10}$	2.2×10^{-10}
M_h[GeV]	[60, 61, 62, 63]	[64, 64]	> 114.4	1.5
$\Omega_{\rm CDM}h^2$	[65, 66, 67]	[3]	0.1099 ± 0.0062	0.012

Table 2: A list of experimental constraints used in `MasterCode`. The values and errors shown are from [46]. `MasterCode` also takes account of the direct SUSY search results at LEP (LEP Supersymmetry Working Group).

function, encompassing experimental constraints and theoretical predictions of the model:

$$\begin{aligned}\chi^2 = & \quad \textstyle\sum_i^N \frac{(C_i-P_i)^2}{\sigma(C_i)^2+\sigma(P_i)^2} \\ + & \quad \chi^2(M_h) + \chi^2(\mathrm{BR}(B_s\to\mu\mu)) \\ + & \quad \chi^2(\text{SUSY search limits}) \\ + & \quad \textstyle\sum_i^M \frac{\left(f^{\rm obs}_{SM_i}-f^{\rm fit}_{SM_i}\right)^2}{\sigma\left(f_{SM_i}\right)^2}\end{aligned}$$

where N is the number of observables, C_i is a measured value[3] and P_i is the corresponding value predicted by our model. The contributions $\chi^2(M_h)$, $\chi^2(\mathrm{BR}(B_s\to\mu\mu))$ and χ^2(SUSY search limits) are from the discrepancy between the model-calculated value of the parameter and current experimental limits. They are separated as the constraint represents only a one-sided limit and not a value, with the third of these being as a result of direct SUSY searches at LEP. Finally, the last (summation) term encompasses the Standard Model paramters $f_{\rm SM} = \{\Delta\alpha_{\rm had}, m_t, M_Z\}$.

[3] A list of experimental constraints can be found in table 2.

In this way for any point in the parameter space we can calculate a confidence limit representing how well the model recreates observables at the electroweak scale. This also has the property of being applicable to any number of models given that the χ^2 probability contains a dependance on the number of degrees of freedom of the model. To expand this idea to providing a method to cover the entire parameter space of a given model a Markov Chain Monte Carlo (MCMC) method is implemented. Here all degrees of freedom of the model are varied simultaneously and a random walk is used to sample the parameter space. While a natural problem arising from implementing random walks MCMCs is inefficiency in exploring the *whole* space (as they proceed randomly through the space and so can easily double/triple cover on long chains), this is easily minimised as a cost in this case by running multiple chains at different points in the parameter space to ensure coverage. This has the added advantage of effectively parallelising the process of sampling.

As stated, the model parameters are varied simultaneously. Once the space has been sampled it is then possible to construct confidence level contours for given parameters. This is calculated by scanning over the desired parameter(s) and minimizing the χ^2 with respsect to the remaining model parameters. More explicity we fix a model parameter ϕ allowing us to determine a χ^2_{min} for the other parameter values. We then vary $\chi^2(\phi)$,

$$\chi^2(\phi) = \chi^2_{\text{min}} + \Delta\chi^2$$

where $\Delta\chi^2$ has values of 2.28(5.99) corresponding to the 68%(95%) confidence limits for our model.

This approach allows the list of constraints to be varied freely, and values can be easily modified, added or removed as applicable. This property makes it possible to investigate a models sensitivity to a given observable/constraint, and their respective errors, allowing the identification of which experimental data have the greatest effect on the model[4]. The method is particularly attractive as it puts no *a priori* constraints on the model parameters themselves as we only care about the models consistency with recreating known observables.

7.1 CMSSM and mSUGRA

At the time of writing scans have been carried out of both the CMSSM and NUHM1[5] [46] parameter spaces using `MasterCode`. Subsequent work has lead to a minimal scan of the mSUGRA space having been carried out. This scan consisted of 780,000 points[6] around the low $m_0, m_{1/2}$ space. Of these points 760,000 were deemed "acceptable". Acceptable points are defined as points where solutions to the renormalization group equations converge. The scan was generated by running multiple markov chains around the area being sampled. A small region around the minimum was sampled to allow comparison to existing model fits (for example the CMSSM) while not requiring coverage of the entire parameter space which is computationally expensive.

It should be noted that the CMSSM scans were carried out while enforcing the LEP constraint on the Higgs mass, M_h, contributing to χ^2 as

$$\chi^2(M_h) = \frac{\left(M_h - M_h^{\text{limit}}\right)^2}{(1.1\text{GeV})^2 + (1.5\text{GeV})^2},$$

Where $M_h^{\text{limit}} = 115.0\text{GeV}$ for $M_h < 115.0$, and points with $M_h > 115.0$ receive no contribution as they are above the limit (see [46] again for more details on this contribution). However, the mSUGRA scan was carried out without this constraint.

[4] see Section 2 of [46] for a discussion of the computational costs involved with resampling an entire mutli-dimensional parameter space

[5] Non-Universal Higgs Model 1, where the masses of the Higgs doublets are allowed to be different from the scalar mass at the GUT scale, $m_1 = m_2 = (m_0 + \Delta M)$

[6] For comparison the CMSSM analysis consisted of ~ 20 million points

mSUGRA minima	χ^2	$m_0[\mathrm{GeV/c^2}]$	$m_{1/2}[\mathrm{GeV/c^2}]$	$A_0[\mathrm{GeV}]$	$\tan\beta$
with $\chi^2(M_h)$	22.1	63.1	318.5	-28.8	8.23
without $\chi^2(M_h)$	21.6	47.9	270.9	7.5	6.17
Δ(param)[%]	2.3	31.7	17.5	-126	33.4
CMSSM minima [46]	20.6	60	310	130	11

Table 3: The minimum χ^2 fit and associated parameters for mSUGRA with and without the LEP M_h penalty constraint. In the mSUGRA case $\tan\beta$ is calculated from the other input parameters. Δ (param) is the change in the mSUGRA best fit-parameter value as percentage of the uncontrained value. The CMSSM best fit is provided for reference.

With this in mind the mSUGRA minimum χ^2 point has been recalculated with the M_h constraint in attempt to understand whether a comparison of the two scans would be valid. The two minima can be seen in table 3. While they both posses relatively similar χ^2 there is a large change in some of the parameters (the largest being a sign change in A_0[7]). However, these changes move the point closer to the CMSSM value, except in A_0.

It is also important to note that all scans are of the $\mu > 0$ parameter space. The $\mu < 0$ case introduces significant problems when trying to resolve the predicted values of $(g-2)_\mu$ and $\mathrm{BR}(b \to s\gamma)$ with the current measurements and limits, generally driving the sparticle spectrum to higher masses.

In all the mSUGRA parameter space plots below the blue contour line represents the 68% confidence contour, and the red line the 95% contour. The general notation for superparticles is to use the normal SM symbol with a tilde overhead, for example the stau is denoted $\tilde{\tau}$.

7.1.1 $m_0, m_{1/2}$ and $\tan\beta, m_0$ parameter spaces

As can be clearly seen in figure 4, once the difference in scale has been taken into account, the focal points in $m_0, m_{1/2}$ are in similar areas of parameter space. The mSUGRA contours are significantly more constrained on the m_0 axis with 68% and 95% contours having ranges, respectively, $[10, 85]$ and $[10, 190]$ whereas in the CMSSM they are $[20, 180]$ and $[20, 800]$. It is natural to expect a reduced contour in the m_0 range given that our model is constrained at the GUT scale by

$$B_0 = A_0 + m_0,$$

and when you take into account that the pseudoscalar higgs mass, M_A, at the tree level is related to B by,

$$M_A^2 = \frac{2B\mu}{\sin 2\beta},$$

this implies that M_A is driven higher by higher m_0.

As one would expect with a lower m_0 range, part of the 68% contour in m_0 covers values of $m_{1/2}$ corresponding to the $\tilde{\chi}_1^0 - \tilde{\tau}_1$ coannihilation region ($m_{1/2} \sim 350\mathrm{GeV/c^2}$ [68] for low m_0) where $m_{\tilde{\chi}_1^0} - m_{\tilde{\tau}_1}$ is small. The minimum calculated is close to satisfying this condition, see figure 7(b) where we predict $m_{\tilde{\chi}_1^0} = 104.4\mathrm{GeV/c^2}$ and $m_{\tilde{\tau}_1} = 116.3\mathrm{GeV/c^2}$ with $m_{1/2} = 270.9\mathrm{GeV/c^2}$, and so likely sits near but under this coannihilation region. This is similar to the CMSSM models where low $\tilde{\chi}_1^0 - \tilde{\tau}_1$ mass differences are preferred [46]. With a larger scan of the parameter space it would be prudent to analyse the relic densities in relation to the known constraints (these fits were produced while constraining the value of $\Omega_\chi h^2$) given the proximity to the coannihilation region to the minima.

While a more constrained parameter space is expected in some regards, we are still at a different order of magnitude of statistics from the CMSSM calculation being used as a comparison. When using MCMC methods the strength of the result is highly dependant on the coverage of the space. While a random walk implementation will always cover the space given enough steps, the data presented here is far from complete and so comparisons on the large scale structure of the parameter space are not possible yet.

[7] It should be noted that it may be difficult to statistically distinguish this value from $A_0 \sim 0$ given the comparatively small statistics, and if $A_0 \simeq 0$ the sign of $A_0^{\min}$ will be of particular importance

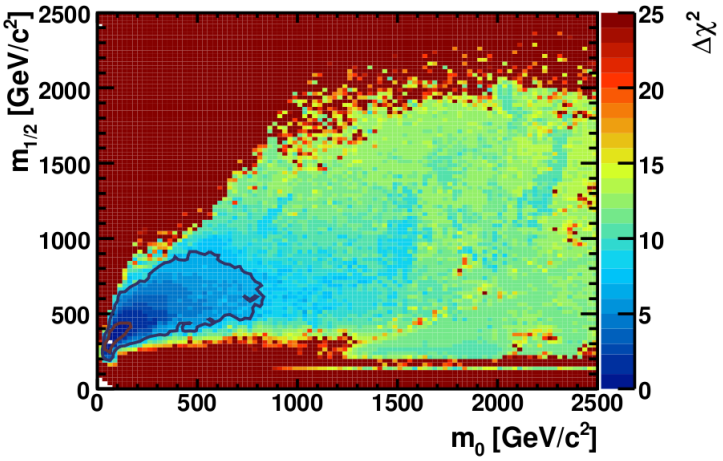

(a) CMSSM

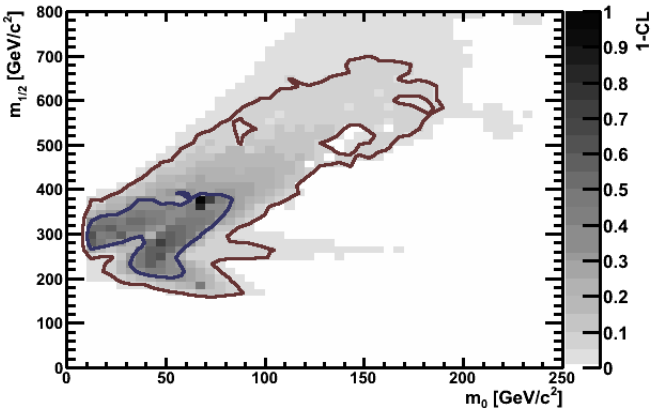

(b) mSUGRA

Figure 4: The m_0,$m_{1/2}$ contours for the CMSSM (top) and mSUGRA (bottom), different axis limits have been used here as a matter of practicality.

It is possible to comment on the structure of specific regions of the parameter space where the coverage was more significant. Fits were started from multiple points in parameter space. None of these points produced $\tan\beta \gtrsim 60$, consistent with the analysis from [20] and the choice of parameter space from [68] for low m_0. We find the minimum point $\tan\beta = 6.17$ ($\tan\beta = 8.23$ with the M_h constraint), with the 68% contour covering $3 < \tan\beta < 11$ and the 95% covering $2 < \tan\beta < 22$ where there are no reasonable points beyond the lower bound. These values, again, show consistency with the bounds on the parameter space discussed in [20].

Both the low edges, in $\tan\beta$ and m_0 are comparable for the CMSSM and mSUGRA cases. For $\tan\beta$ this is expected as points with $\tan\beta < 2$ tend to be associated with numerical instabilities when attempting to converge the renormalization group equations. The upper limits in mSUGRA are largely reduced from that of the CMSSM analysis. The observed $\tan\beta < 22$ is also consistent with the analysis of [20], and can be better understood in terms of figure 8 discussed in Section 7.1.3. The limit $m_0 \lesssim 200\text{GeV/c}^2$ is best understood by considering the original boundary condition that defines mSUGRA,

$$m_0^2 = m_{3/2}^2 + \cancel{A}^0 \Rightarrow m_0 = m_{3/2},$$

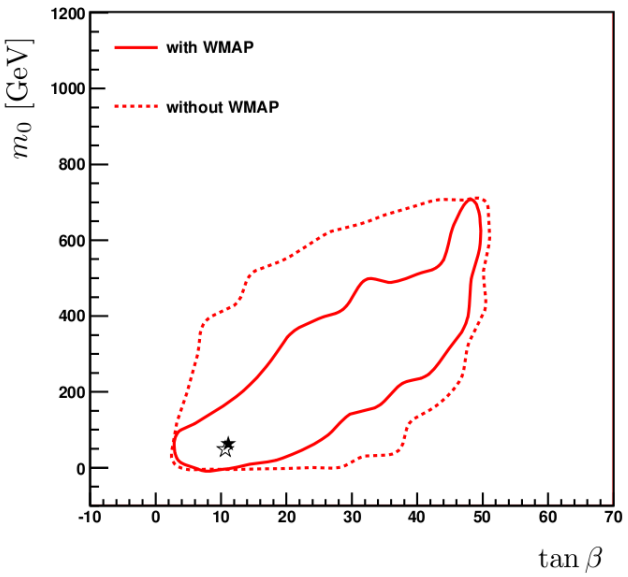

(a) CMSSM

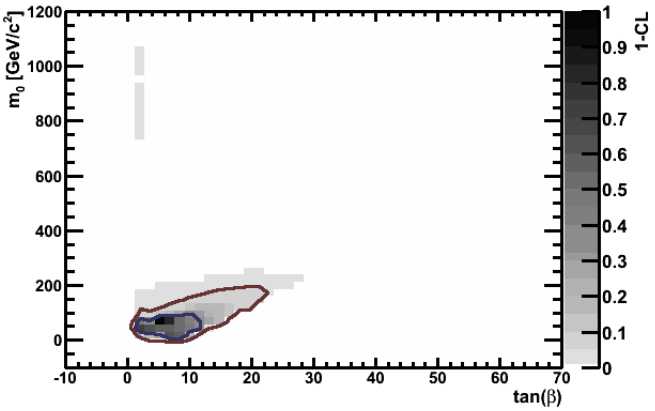

(b) mSUGRA

Figure 5: The tan (β), m_0 contour(s) for the CMSSM (top, no M_h constraint, 95% contour only, where WMAP refers to the WMAP relic dark matter density constraint) [70] and mSUGRA (bottom).

so higher m_0 corresponds to a higher gravitino mass, and in the Gravitino Dark Matter scenario (GDM) this results in a poor fit to our constraints [69]. The application of our constraints to the GDM scenario is discussed in more detail in section 7.1.4.

7.1.2 Higgs mass likelihoods

While the LEP constraint on M_h hasn't been enforced in these fits, the value corresponding to the minimum point with this constraint enforced has been calculated. The important features in figure 6 are not just the minimum value but the behaviour in the neighbourhood of the minimum, in particular the value of $\Delta\chi^2$ as $M_h > M_h^{\mathrm{LEP}}$.

With no constraint we find a minimum χ^2 for $M_h = 111.47\mathrm{GeV/c}^2$, crossing the LEP constraint with $\Delta\chi^2 = 0.6$. With the constraint applied we find $M_h = 114.52\mathrm{GeV/c}^2$ with a marginally raised χ^2_{min}. In the CMSSM case the constrained (unconstrained) values are $M_h \lesssim 114\,(110)\,\mathrm{GeV/c}^2$ with $\Delta\chi^2 \sim 0.2\,(2)$. This suggests that mSUGRA models are subject to the same tension between the fit results and the direct

search limits as the CMSSM. We also observe that mSUGRA models seem to prefer a higher Higgs mass than that of the CMSSM, and when carrying out the full parameter-space scan it will be revealing to determine if this is a general property of mSUGRA.

The $\Delta\chi^2$ behaviour with $M_h > M_h\left(\chi^2_{\text{min}}\right)$ is similar in both models, with both reaching $\Delta\chi^2 = 6$ for $M_h \simeq 120$ GeV/c^2. For $M_h < M_h\left(\chi^2_{\text{min}}\right)$ the mSUGRA model shows a slightly more rapid increase in χ^2 with $\Delta\chi^2 = 6$ for $M_h = 88.5$ GeV/c^2, with the CMSSM having $M_h = 84$ GeV/c^2. Though it is important to notice the difference in scale of the $\Delta\chi^2$-axes, as they both have similar rates of change of $\Delta\chi^2$ at this point.

Both figure 6(b) and the unconstrained line in figure 6(a) show some small deviations in the line (a marked change in $\frac{\partial^2(\Delta\chi^2)}{\partial(M_h)^2}$) around both $M_h \simeq 90$ and 100GeV/c^2). Though the origin of this behaviour is not understood currently, and with the reduced statistics of the mSUGRA scan it is impossible to comment on whether this is a 'real' effect, with more statistics the cause of these deviations (if they remain) needs to be investigated. It is possible that this is an edge-effect from reduced statistics in both models, where it is unlikely that one generates points with the necessary Higgs masses to populate (and smooth) the plots.

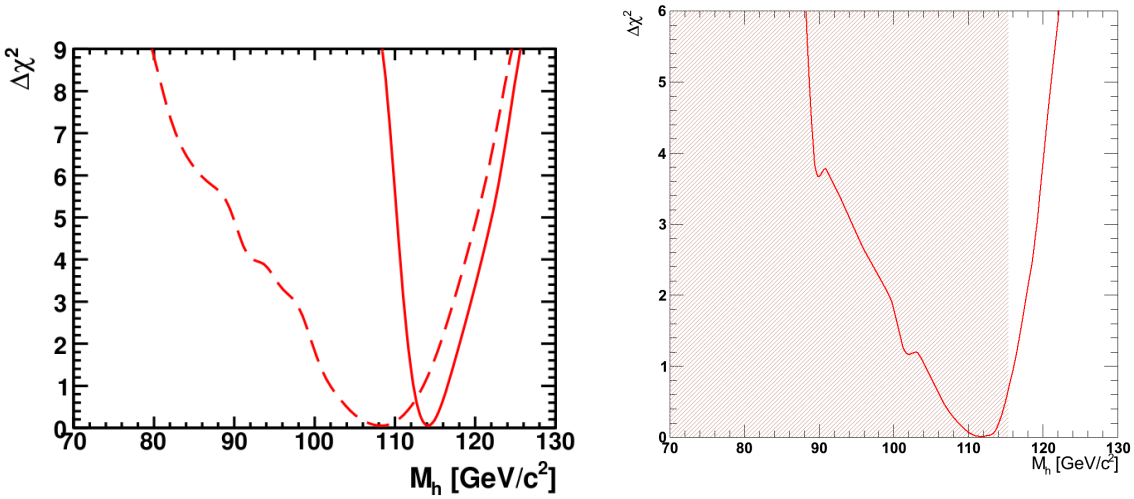

(a) CMSSM (b) mSUGRA

Figure 6: The likelihood functions for M_h in the CMSSM(left) solid(dashed) line with(without) LEP constraint and mSUGRA(right, no constraint applied) with constrained region shaded for reference.

7.1.3 Sanity checks

While comparisons to the CMSSM minima and space reveal similarities and can help us understand the mSUGRA parameter space, it is important that we are producing reliable results and that any similarities/differences are truly part of the model. Fortunately, while no full scan of the parameter space has been carried out, the mSUGRA model is well understood both theoretically and pheomenologically.

As part of the work at the Compact Muon Solenoid (CMS), at the LHC, aimed at revealing the first signs of supersymmetry, benchmark test points have been developed for the MSSM and subsequently adopted for mSUGRA [71]. The minimum χ^2 point for mSUGRA calculated here lies close to one of the low mass benchmark points LM1. This point has the values $m_0 = 60$ GeV/c^2, $m_{1/2} = 200$ GeV/c^2 and $A_0 = 0$ GeV. Given that it is comparable in all three input parameters to our minimum, we would expect very similar sparticle masses and resulting phenomenology. This can serve as effective sanity check for our implementation of the mSUGRA model, given that the LM1 point is well studied, we should accurately recreate the spectrum of sparticle masses.

Shown in figure 7 are the comparative sparticle spectra for both the LM1 benchmark point and the mSUGRA minimum χ^2 point presented here. An initial inspection shows good agreement, and barring one small change, the hierarchy is identical. In the LM1 case the three lighest partners (from heaviest to lightest are) $h^0, \tilde{\tau}_1$ and $\tilde{\chi}_1^0$. In the mSUGRA case they are $\tilde{\tau}_1, h^0$ and $\tilde{\chi}_1^0$, where the actual mass difference in the particles between LM1 and our minimum is small but the mass splitting of the sfermions is larger at LM1. Both hierarchies show the heaviest partner to be the gluino, $\tilde{g}$, with LM1 showing $m_{\tilde{g}} \gtrsim 600$ GeV/c^2 and mSUGRA $m_{\tilde{g}} \gtrsim 650$ GeV/c^2. In the mSUGRA case all sparticles are at least marginally more massive than the equivalent calculated at LM1.

It should be noted that there is a particle missing from both the spectra presented, the gravitino $\tilde{G}$. It's position and the reason for exclusion will be commented on in Section 7.1.4.

A second check we can make on the validity of the calculations is comparing point like scans to more general characterizations of the parameter space. One can define,

$$\begin{aligned} A_0 = &\quad \hat{A} m_0 \\ B_0 = &\quad \hat{B} m_0 \end{aligned}$$

as in [20]. Our boundary condition becomes,

$$\hat{B} = \hat{A} + 1.$$

It is possible for certain values of $\hat{A}$ and $\hat{B}$ to calculate the allowed ranges of $\tan\beta$ while using a small number of phenomenological constraints as demonstrated in [20]. Figure 8(a) shows these allowed values of $\tan\beta$ for varying $\hat{A}$ which characterises two of our input parameters. By comparing this to the likelihood plot in figure 8(b) we see that the bulk behavior is similar, but in particular the actual minimum ($\hat{A} = -0.15, \tan\beta = 6.17$ in this sign convention) lies in the middle of this allowed range.

While there seems to be part of the contour that lies outside of the range shown in 8(a) this can, in part, be explained by returning to the M_h constraint. The allowed range in figure 8(a) was calculated by strictly constraining $M_h > 114$ GeV/c^2, whereas our contours have no M_h constraint implemented. Whether this difference is significant or not will be resolved when a full scan implementing the Higgs mass constraint is completed.

7.1.4 LSPs

As already discussed the gravitino has thus far been ignored in considerations (see the spectra in figure 7). As also disucssed, the results presented are at the early stage of the scan of mSUGRA parameter space, and the machinery to fully analyse the reasonable phenomenology of this has not yet been implemented.

The essential part of the defining condition of mSUGRA is $m_0 = m_{3/2}$. This is particularly relevant when determining the LSP. Consider that

$$m_{1/2} \sim \underbrace{2.5 m_{\tilde{\chi}_1^0} < 2.5 m_{3/2}}_{\text{If } \tilde{\chi}_1^0 \text{ LSP}} = 2.5 m_0$$

recalling that $\tilde{\chi}_1^0$ is approximately just the Bino (superpartner to the weak-hypercharge gauge field). This gives us a rough way of discriminating between points with a neutralino LSP and a gravitino LSP.

$$\begin{aligned} m_{1/2} \lesssim 2.5 m_0 \Rightarrow &\quad m_0 > m_{\tilde{\chi}_1^0} \Rightarrow \tilde{\chi}_1^0 \text{ LSP} \\ m_{1/2} \gtrsim 2.5 m_0 \Rightarrow &\quad m_0 < m_{\tilde{\chi}_1^0} \Rightarrow \tilde{G} \text{ LSP} \end{aligned}$$

Recall that one of the constraints applied, listed in table 2, was on the cold dark matter relic abundance $\Omega_{\text{CDM}} h^2$. However this constraints is *only* applicable in the case of a $\tilde{\chi}_1^0$ LSP, and that for $\tilde{G}$ LSP $\Omega_{\text{CDM}} h^2$ is irrelevant. Instead in this case we only care about the relic density of gravitinos, $\Omega_{\tilde{G}} h^2$ and astrophysical constraints on the decay of $\tilde{\chi}_1^0 \to \tilde{G}$.

This concern becomes particularly relevant when we return to the calculated minimum point, where we see that $\frac{m_{1/2}}{m_0} = 5.66$, placing it clearly in the gravitino dark matter region of parameter space, and means the application of the $\Omega_{\text{CDM}}h^2$ constraint was in error. Though initial investigations show that removing this may not drastically change the parameter space it will have an effect on the location and value of the minimum χ^2 as well as possibly opening up areas of the space that were ruled out in the CMSSM case [72].

8 Conclusion and outlook

We have introduced and motivated several models of supersymmetry that provide reasonable and consistent behaviour at the electroweak scale. In particular an analysis of minimal supergravity has been presented and the area of parameter space most consistent with current observables is identified. The result of this analysis seems to pass comparison tests to both benchmark points for supersymmetry as well as to other, more specific, analysis results. This would seem to validate the method used here, but as discussed further testing with a higher coverage of the parameter space is necessary.

In particular we note that while, here, a constraint on cold dark matter denisty was applied this is not always relevant to this model and as such the parameter space scan should be revisited in more detail. However, even taking this into account we only expect this to allow reasonable behaviour in a larger region of parameter space but not drastically alter the minimum χ^2 point. Therefore we still expect the minimum point to be located near the LM1 benchmark point.

Overall this serves as a further test of our method when applied to SUSY models that implement boundary conditions at the GUT scale. This method can be particularly useful when trying to do comparisons between the favoured phenomenology of different models. Using this method we can both find the points in parameter space that are most consistent with current observations as well as defining particle spectra and phenomenological behaviour. In essense, this provides us a tool with which to characterise models of supersymmetry which can aid in disintguishing which model may be responsible for any signals that are seen in the data taken at the LHC.

As discussed, our minimum points for our models are in proximity to one of the low mass benchmark points for SUSY, as is most of the 68% contour (as demonstrated for the mSUGRA parameter space). This is a particularly interesting result as it presents the possibility of early discovery in the data from the LHC. Not only this, but a large proportion of the parameter spaces are within the reach of the LHC's energy range. Lacking any discovery would also have a strong impact on these models, excluding regions and thereby cutting away parts of the parameter space. Future work will be targetted at combining the results of SUSY searches from the LHC with theoretical models. Ultimately this can help us realise what are plausible models of supersymmetry.

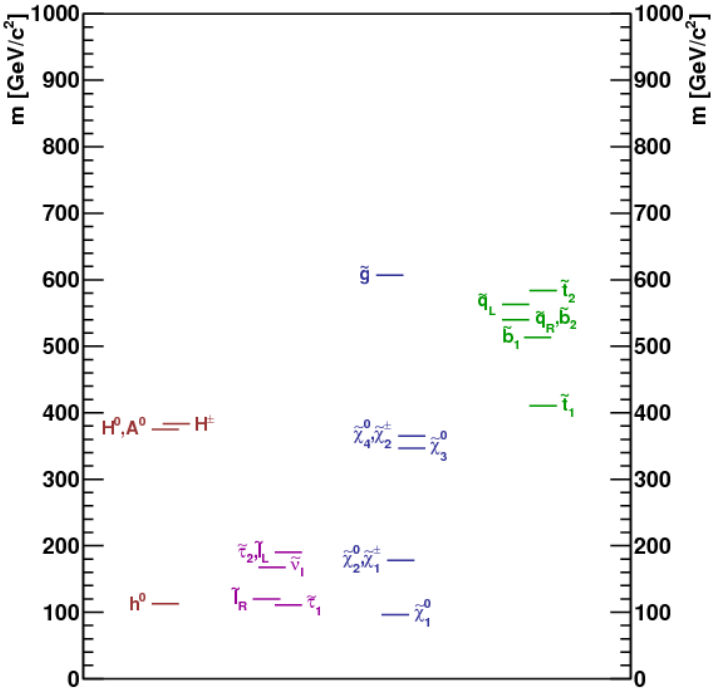

(a) LM1 Benchmark

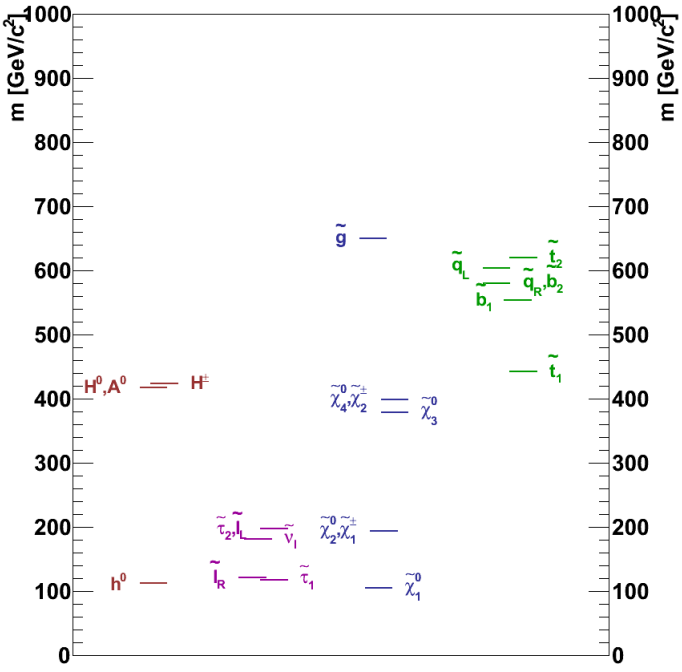

(b) mSUGRA

Figure 7: Comparative particle spectra for the LM1 mSUGRA benchmark point (top) and the `MasterCode` identified minimum in mSUGRA (bottom).

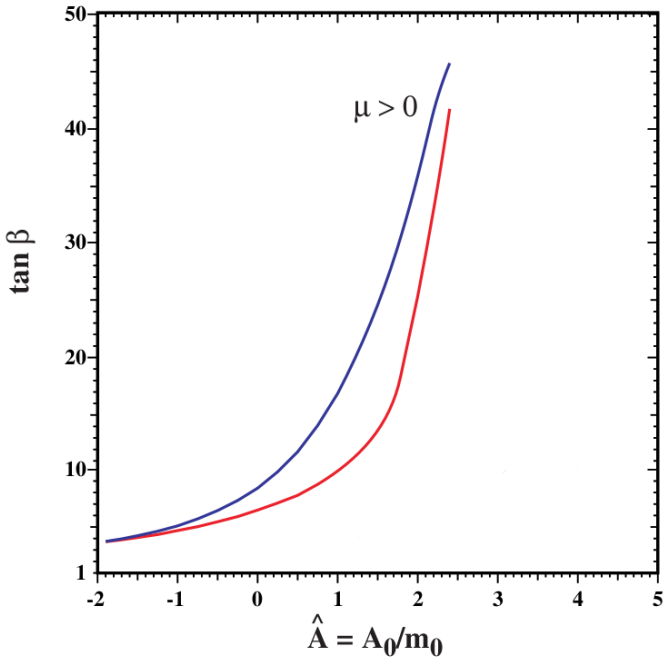

(a) mSUGRA limits

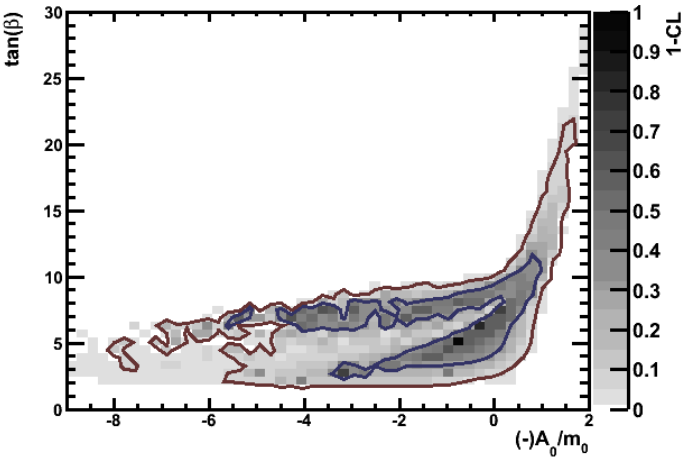

(b) mSUGRA Likelihood

Figure 8: The allowed values of $\tan\beta$ for varying A_0/m_0(top) [20] and the corresponding mSUGRA parameter space (bottom). The calculations here have used the opposite sign convention to that in [20] and so for clarity this has been reversed in figure 8(b).

References

[1] P. W. Higgs, Phys. Rev. Lett. **13**, 508 (1964).

[2] D. N. Spergel *et al.*, The Astrophysical Journal Supplement Series **148**, 175 (2003).

[3] WMAP, J. Dunkley *et al.*, Astrophys. J. Suppl. **180**, 306 (2009), arXiv:astro-ph/0803.0586.

[4] J. Ellis, K. A. Olive, and E. Vangioni, Physics Letters B **619**, 30 (2005), arXiv:astro-ph/0503023.

[5] D. McKeen, Contributions to the Muon's Anomalous Magnetic Moment from a Hidden Sector, 2009, arXiv:hep-ph/0912.1076.

[6] B. E. Lautrup and E. de Rafael, Phys. Rev. **174**, 1835 (1968).

[7] Vogel, M. *et al.*, Eur. Phys. J. Special Topics **163**, 113 (2008).

[8] B. L. Roberts, (2010), arXiv:hep-ex/1001.2898.

[9] G. Passarino, Nuclear Physics B **343**, 31 (1990).

[10] J.F. Gunion, A. Stange, S. Willenbrock, *Electroweak Symmetry Breaking and new physics at the TeV scale* (World Scientific, 1996).

[11] S. L. Glashow and S. Weinberg, Phys. Rev. D **15**, 1958 (1977).

[12] ALEPH Collaboration, DELPHI Collaboration, L3 Collaboration, OPAL Collaboration, and The LEP Working Group For Higgs Boson Searches, Physics Letters B **565**, 61 (2003), arXiv:hep-ex/0306033.

[13] On behalf of the CDF, M. Lancaster, (2010), arXiv:hep-ex/1005.5509.

[14] J. Alwall, P. C. Schuster, and N. Toro, (2009), arXiv:hep-ph/0810.3921v2.

[15] N. Arkani-Hamed, S. Dimopoulos, and G. Dvali, Phys. Rev. D **59**, 086004 (1999).

[16] P. Langacker and N. Polonsky, Phys. Rev. D **47**, 4028 (1993).

[17] O. Buchmueller *et al.*, Phys. Lett. **B657**, 87 (2007), arXiv:hep-ph/0707.3447.

[18] M. Bustamante, L. Cieri, and J. Ellis, (2009), arXiv:hep-ph/0911.4409.

[19] A. Brignole, L. E. Ibanez, and C. Munoz, (1997), arXiv:hep-ph/9707209.

[20] J. Ellis, K. A. Olive, Y. Santoso, and V. C. Spanos, Physics Letters B **573**, 162 (2003), arXiv:hep-ph/0305212.

[21] O. Antipin and K. Tuominen, Physical Review D **79**, 075011 (2009), arXiv:hep-ph/0901.4243.

[22] The CMS Collaboration, CMS PAS 2008/038 (2009).

[23] M. Chiorboli, M. Galanti, and A. Tricomi, Report No. CMS-CR-2006-037. CERN-CMS-CR-2006-037, 2006 (unpublished).

[24] J. Mrazek and A. Wulzer, (2009), arXiv:hep-ph/0909.3977.

[25] H. Flaecher *et al.*, CMS-AN-2009-056 (CMS internal note).

[26] R. Trotta, F. Feroz, M. Hobson, L. Roszkowski, and R. Ruiz de Austri, Journal of High Energy Physics **12**, 24 (2008), arXiv:hep-ph/0809.3792.

[27] S. Heinemeyer, W. Hollik, D. Stöckinger, A. M. Weber, and G. Weiglein, Journal of High Energy Physics **8**, 52 (2006), arXiv:hep-ph/0604147.

[28] S. Heinemeyer, W. Hollik, A. M. Weber, and G. Weiglein, Journal of High Energy Physics **4**, 39 (2008), arXiv:hep-ph/0710.2972.

[29] Tevatron Electroweak Working Group, for the CDF Collaboration, and the D0 Collaboration, ArXiv e-prints (2009), arXiv:hep-ex/0903.2503.

[30] The ALEPH Collaboration *et al.*, Phys Rept **427**, 257 (2006), arXiv:hep-ex/0509008.

[31] M. Verzocchi, talk at ICHEP 2008 (August 2008).

[32] LEP Electroweak Working Group, http://lepewwg.web.cern.ch/LEPEWWG/Welcome.html .

[33] M. Misiak *et al.*, Physical Review Letters **98**, 022002 (2007), arXiv:hep-ph/0609232.

[34] M. Ciuchini, G. Degrassi, P. Gambino, and G. F. Giudice, Nuclear Physics B **534**, 3 (1998), arXiv:hep-ph/9806308.

[35] G. Degrassi, P. Gambino, and G. F. Giudice, Journal of High Energy Physics **12**, 9 (2000), arXiv:hep-ph/0009337.

[36] M. Carena, D. Garcia, U. Nierste, and C. E. M. Wagner, Physics Letters B **499**, 141 (2001), arXiv:hep-ph/0010003.

[37] G. D'Ambrosio, G. F. Giudice, G. Isidori, and A. Strumia, Nuclear Physics B **645**, 155 (2002), arXiv:hep-ph/0207036.

[38] Heavy Flavor Averaging Group *et al.*, ArXiv High Energy Physics - Experiment e-prints (2006), arXiv:hep-ex/0603003.

[39] G. Isidori and A. Retico, Journal of High Energy Physics **11**, 1 (2001), arXiv:hep-ph/0110121.

[40] A. J. Buras, P. H. Chankowski, J. Rosiek, and L. Slawianowska, Nuclear Physics B **659**, 3 (2003), arXiv:hep-ph/0210145.

[41] G. Isidori and P. Paradisi, Physics Letters B **639**, 499 (2006), arXiv:hep-ph/0605012.

[42] G. Isidori, F. Mescia, P. Paradisi, and D. Temes, Physical Review D **75**, 115019 (2007), arXiv:hep-ph/0703035.

[43] A. G. Akeroyd and S. Recksiegel, Journal of Physics G Nuclear Physics **29**, 2311 (2003), arXiv:hep-ph/0306037.

[44] M. Antonelli *et al.*, ArXiv e-prints (2009), arXiv:hep-ph/0907.5386.

[45] A. Gray *et al.*, Physical Review Letters **95**, 212001 (2005), arXiv:hep-lat/0507015.

[46] O. Buchmueller *et al.*, European Physical Journal C **64**, 391 (2009).

[47] C. Bobeth, A. J. Buras, and T. Ewerth, Nuclear Physics B **713**, 522 (2005), arXiv:hep-ph/0409293.

[48] The Flavianet Kaon Working Group, B. Sciascia, and the FlaviaNet Kaon Working Group*, Nuclear Physics B Proceedings Supplements **181**, 83 (2008), arXiv:hep-ph/0801.1817.

[49] A. J. Buras, P. Gambino, M. Gorbahn, S. Jäger, and L. Silvestrini, Nuclear Physics B **592**, 55 (2000), arXiv:hep-ph/0007313.

[50] A. V. Artamonov *et al.*, Physical Review Letters **101**, 191802 (2008), arXiv:hep-ex/0808.2459.

[51] V. Lubicz and C. Tarantino, Nuovo Cimento B Serie **123**, 674 (2008), arXiv:hep-lat/0807.4605.

[52] M. Bona *et al.*, Journal of High Energy Physics **3**, 49 (2008), arXiv:hep-ph/0707.0636.

[53] T. Moroi, Phys. Rev. **D53**, 6565 (1996), arXiv:hep-ph/9512396.

[54] G. Degrassi and G. F. Giudice, Phys. Rev. **D58**, 053007 (1998), arXiv:hep-ph/9803384.

[55] S. Heinemeyer, D. Stockinger, and G. Weiglein, Nucl. Phys. **B690**, 62 (2004), arXiv:hep-ph/0312264.

[56] S. Heinemeyer, D. Stockinger, and G. Weiglein, Nucl. Phys. **B699**, 103 (2004), arXiv:hep-ph/0405255.

[57] Muon G-2, G. W. Bennett *et al.*, Phys. Rev. **D73**, 072003 (2006), arXiv:hep-ex/0602035.

[58] M. Davier, Nucl. Phys. Proc. Suppl. **169**, 288 (2007), arXiv:hep-ph/0701163.

[59] D. W. Hertzog, J. P. Miller, E. de Rafael, B. Lee Roberts, and D. Stockinger, (2007), arXiv:hep-ph/0705.4617.

[60] G. Degrassi, S. Heinemeyer, W. Hollik, P. Slavich, and G. Weiglein, Eur. Phys. J. **C28**, 133 (2003), arXiv:hep-ph/0212020.

[61] S. Heinemeyer, W. Hollik, and G. Weiglein, Eur. Phys. J. **C9**, 343 (1999), arXiv:hep-ph/9812472.

[62] S. Heinemeyer, W. Hollik, and G. Weiglein, Comput. Phys. Commun. **124**, 76 (2000), arXiv:hep-ph/9812320.

[63] M. Frank *et al.*, JHEP **02**, 047 (2007), arXiv:hep-ph/0611326.

[64] ALEPH, S. Schael *et al.*, Eur. Phys. J. **C47**, 547 (2006), arXiv:hep-ex/0602042.

[65] G. Belanger, F. Boudjema, A. Pukhov, and A. Semenov, Comput. Phys. Commun. **176**, 367 (2007), arXiv:hep-ph/0607059.

[66] G. Belanger, F. Boudjema, A. Pukhov, and A. Semenov, Comput. Phys. Commun. **149**, 103 (2002), arXiv:hep-ph/0112278.

[67] G. Belanger, F. Boudjema, A. Pukhov, and A. Semenov, Comput. Phys. Commun. **174**, 577 (2006), arXiv:hep-ph/0405253.

[68] R. Arnowitt, B. Dutta, and Y. Santoso, Nuclear Physics B **606**, 59 (2001), arXiv:hep-ph/0102181.

[69] S. Heinemeyer, Pramana **69**, 947 (2007), arXiv:hep-ph/0611372.

[70] O. Buchmueller *et al.*, Journal of High Energy Physics **9**, 117 (2008), arXiv:hep-ph/0808.4128.

[71] M. Battaglia *et al.*, European Physical Journal C **33**, 273 (2004), arXiv:hep-ph/0306219.

[72] J. Ellis, K. A. Olive, Y. Santoso, and V. C. Spanos, Physics Letters B **588**, 7 (2004), arXiv:hep-ph/0312262.